White Dwarfs as Probes of Fundamental Physics: Tracers of Planetary, Stellar and Galactic Evolution
Proceedings IAU Symposium No. 357, 2019
M. A. Barstow, S. J. Kleinman, J. L. Provencal & L. Ferrario, eds.
doi:10.1017/S1743921320000216

Geometry of nova ejecta

M. Pavana[1,2], G. C. Anupama[1], Ramya M. Anche[1], U. S. Kamath[1] and G. Selva Kumar[1]

[1]Indian Institute of Astrophysics, Koramangala block II, 560034 Bangalore, India
[2]Pondicherry University, R. V. Nagar, Kalapet, 605014 Puducherry, India
email: pavana@iiap.res.in, murali.pavana@gmail.com

Abstract. We present photo-ionization and morpho-kinematic analyses of the ejecta of novae. The sample consists of ten novae belonging to the Fe II, He/N and hybrid classes. The Fe II class of novae in the sample have bipolar cone-like structures, with or without equatorial rings with inclination angle in the range of 40°–60°. The He/N novae have bullet-nose curve along with bipolar cone-like structures and equatorial rings with an inclination angle of ∼80°. The hybrid nova in the sample is a bipolar frustum of prolate spheroid along with bipolar cone-like structures and equatorial rings with an inclination angle of 63°.

Keywords. novae, cataclysmic variables - stars : individual - techniques : spectroscopic

1. Introduction

Geometry of nova ejecta provides useful information on the nature of the binary system. The complex structures in the ejecta are not well understood. These may be formed as a consequence of several mechanisms such as interaction of the outflow from white dwarf (WD) with the secondary, rotation of the WD, prominent magnetic field of the WD, and interaction of the ejecta with a pre-existing circumbinary material. A sample of ten novae is used here to understand the geometry of nova ejecta. Seven novae among these belong to Fe II class and two to He/N and one to the hybrid class of nova. The details of the sample are given in Table 1. The novae in the sample are also those with distinct features such as γ-ray emission, ^{7}Be II detection, secondary maxima or few rebrightenings in the optical light curve, complex velocity profiles, dust formation and observational evidence of pre-existing circumbinary material.

The optical spectra used in this study are obtained using the Himalayan Faint Object Spectrograph Camera (HFOSC) with R = 1300 and 2200, and the Hanle Echelle Spectrograph (HESP) with R = 30000 and 60000 at the 2 m Himalayan Chandra Telescope (HCT), and the high resolution echelle spectrograph with R = 27000 at the 2.3 m Vainu Bappu Telescope (VBT).

2. Analyses

The photo-ionization code CLOUDY, C17.01 (Ferland *et al.* 2017) was used to model the low resolution optical spectra. The 3D ionization structure of the ejecta was obtained using pyCloudy (Morisset 2013), as described in Pavana *et al.* (2019). The morpho-kinematic application, SHAPE (Steffen *et al.* 2011) was used to analyse and understand the morphological geometry of the nova ejecta using Hα velocity profiles. The morphologies obtained for all the novae are as shown in Figs. 1 and 2.

Table 1. Details of individual objects in the sample.

Object	Date	Days since discovery	Type	Resolution	Lines used	Analysis
V339 Del	23 Sept 2013	39	Fe II	27000	Hα	Morpho-kinematic
V1369 Cen	22 Dec 2013	20	Fe II	27000	Hα	Morpho-kinematic
V5857 Sgr	12 Apr 2018	04	Fe II	30000	Hα	Morpho-kinematic
V3665 Oph	10 Mar 2018	05	Fe II	60000	Hα	Morpho-kinematic
V5587 Sgr	06 Jun 2011	132	Fe II	1300	Hα	Morpho-kinematic
V2362 Cyg	25 Jul 2007	480	Fe II	1300	He I, He II, [O I], [O III], [N II], Hα, Hβ	Photo-ionization
V2944 Oph	24 Feb 2017	699	Fe II	1300	He I, He II, [O III], [N II], Hα, Hβ	Photo-ionization
V477 Sct	23 Nov 2005	43	He/N	1300, 2200	He I, He II, [O III], [N II], Hα, Hβ	Photo-ionization
M31N 2008-12a	08 Nov 2018	1.8	He/N	1300	He I, He II, [N II], Hα, Hβ	Photo-ionization
V5588 Sgr	09 May 2011	43	Hybrid	1300, 2200	Fe II, He I, He II, [O I], [N II], Hα, Hβ	Photo-ionization

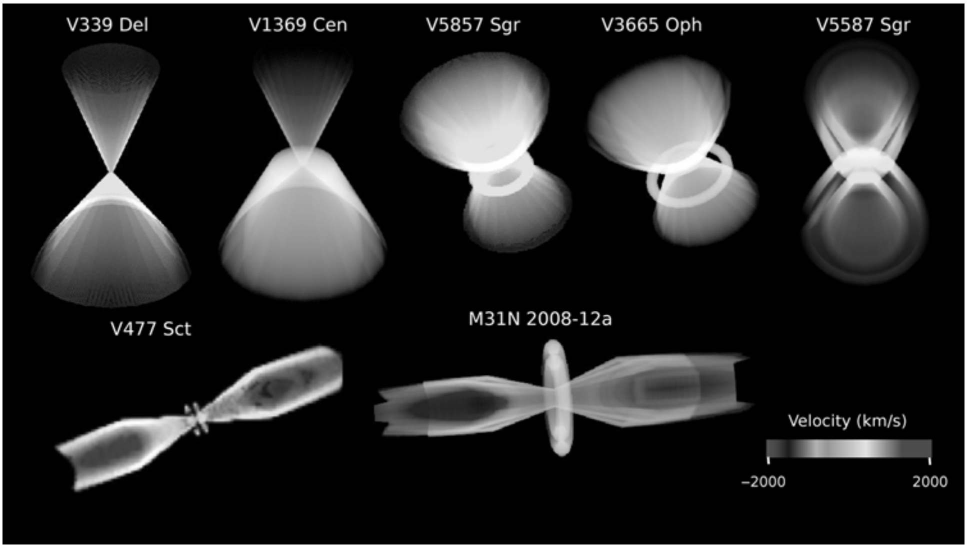

Figure 1. Morphology of the nova ejecta generated using Hα velocity profiles as seen in SHAPE corresponding to their inclination angles.

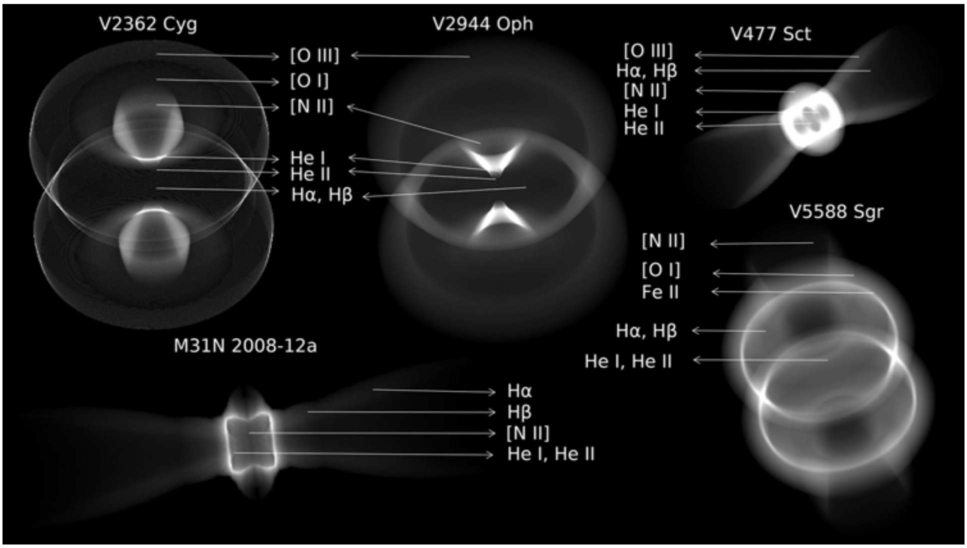

Figure 2. Ionized geometrical structure of nova ejecta generated using the optical spectrum corresponding to their inclination angles.

3. Discussion

In order to understand the mechanisms resulting in the formation of complex structures of nova ejecta, a sample of ten novae was considered. A robust model is required for novae to understand the complex velocity profiles. This can be achieved by choosing a sample with different characteristic features seen in the system as it evolves.

It was suggested by Ribeiro *et al.* (2013a) that morphology of He/N type, Nova Mon 2012 is bipolar with a high inclination angle of 82° ± 6°. The best-fitting remnant morphology of He/N type, Nova Cyg 2008 #2, was found to be polar blobs and an equatorial ring with an high inclination angle of 80° by Ribeiro *et al.* (2011). The best-fit

https://doi.org/10.1017/S1743921320000216 Published online by Cambridge University Press

Table 2. Geometry of nova ejecta.

Object	Type	i (°)	Morphology	Comments
V339 Del	Fe II	58	Asymmetric bipolar cones	Asymmetry is attributed to the optical depth effects (Ribeiro *et al.* 2011) as the system is still in its early decline phase.
V1369 Cen	Fe II	50	Asymmetric bipolar cones	
V5857 Sgr	Fe II	41	Asymmetric bipolar cones with an equatorial ring	Asymmetry attributed to the optical depth effects as the system is in the optical maximum phase where the optical depth is higher, fast moving material at this angle could give rise to equatorial ring (Ribeiro *et al.* 2011).
V3665 Oph	Fe II	45	Asymmetric bipolar cones with an equatorial ring	
V5587 Sgr	Fe II	54	Bipolar cones	Almost symmetric structure and cones might be due to the interaction of wind with the secondary (Gill *et al.* (1999) and O'Brien *et al.* (1995)).
V2944 Oph	Fe II	51	Bipolar cones with equatorial rings	Equatorial ring due to the interaction of the outflow with pre-existing circumbinary material (Munari & Walter 2016).
V2362 Cyg	Fe II	48	Bipolar frustum of prolate spheroid, bipolar cones with equatorial rings	Origin of forbidden lines like [O III] and [N II] is found to be from the outer regions implying that it is coming from the optically thin expanding shell as rightly known that they do not come from primary, secondary or the accretion disc.
V477 Sct	He/N	83	Bullet-nose curve, bipolar cones with equatorial rings	Helium lines are coming from the accretion disc.
M31N 2008-12a	He/N	81	Bullet-nose curve, bipolar cones with an equatorial ring	Helium lines are coming from the inner regions of common envelope.
V5588 Sgr	Hybrid	63	Bipolar frustum of prolate spheroid, bipolar cone-like with equatorial rings	[N II] structure may be generated as a consequence of frictional interaction of wind with the secondary. Presence of equatorial ring due to low expansion ejecta velocity of Fe II lines (Lloyd *et al.* 1997).

i – inclination angle, angle between the ejecta axis and line of sight.

Hα profile corresponding to the observed profile of KT Eri obtained by Ribeiro *et al.* (2013b) resulted in a dumbbell shaped structure with an inclination angle of 58°. The ionized structure of the ejecta of the well-known RN of hybrid class, T Pyx, was found to be a bipolar conical structure with equatorial rings with a low inclination angle of ∼15° (Pavana *et al.* 2019). The best-fit morphology of the hybrid nova, V906 Car was found to be asymmetric bipolar blob-like structure with an inclination angle of about 53° (Pavana *et al.* [in preparation]).

There is a clear distinction between the morphologies obtained for Fe II, He/N and hybrid class of novae (Table 2). This indicates that it evidently depends on the ejecta mechanism. However, confirmation on this can be obtained only after increasing the sample. One interesting feature seen in all novae in the sample is the presence of cone-like structures. From the numerical calculations and suggestions in the literature by Gill *et al.* (1999) and O'Brien *et al.* (1995), cones are generated as a consequence of frictional interaction of wind with the secondary, and rings as a consequence of sweeping up conical regions of enhanced density in the ejected mass from the primary. In the case of HR Del, Hutchings (1972) suggested the sharp and low velocity of the central peaks in the line profile are an indication of an inner cone of low velocity, either with a small cone angle, or viewed pole-on, while equatorial ring gives rise to less-sharp peaks and a more filled-in profile, even when it is thin. It is noticed from our sample that [N II] emission is from the equatorial ring components in the case of V477 Sct and also T Pyx (Pavana *et al.* 2019), rather than from the bipolar regions as in the case of V5588 Sgr. This might be due to variation in ionization rather than the density as also seen and suggested in the case of V705 Cas by Gill *et al.* (1999).

4. Summary

The important results are summarised as follows.

(*a*) The Fe II class of novae in our sample have bipolar cone-like structures with or without equatorial rings with inclination angle in the range of 40° − 60°.

(*b*) The He/N novae have bullet-nose curve along with bipolar cone-like structures and equatorial rings with an inclination angle of ∼80°.

(*c*) The hybrid nova in the sample (V5588 Sgr) is a bipolar frustum of prolate spheroid along with bipolar cone-like structures and equatorial rings with an inclination angle of 63°.

(*d*) This study suggests there could be some differences in the ejecta mechanism for the different types of novae.

References

Ferland, G. J. *et al.* 2017, *ArXiv preprint*, (arXiv:1705.10877)

Gill, C. D. & O'Brien, T. J. 1999, *MNRAS*, 307, 677

Hutchings, J. B. 1972, *MNRAS*, 158, 177

Morisset, C. 2013, *Astrophysics Source Code Library* (ascl:1304.020)

Munari, U. & Walter, F. M. 2016, *MNRAS*, 455, L57

Lloyd, H. M., O'Brien, T. J., & Bode, M. F. 1997, *MNRAS*, 284, 137

O'Brien, T. J., Lloyd, H. M., Slavin A. J., *et al.* 1995, in Harpaz A., Soker N., eds, *Annals of the Israel Physical Society* Vol. 11, Asymmetrical Planetary Nebulae. p. 258

Pavana, M., Anche, R. M., Anupama, G. C., Ramaprakash, A. N., Selvakumar, G., *et al.* 2019, *A&A*, 622, A126

Ribeiro, V. A. R. M. *et al.* 2011, *MNRAS*, 412, 1701

Ribeiro, V. A. R. M., Munari U., Valisa P. *et al.* 2013a, *ApJ*, 768, 49

Ribeiro, V. A. R. M. *et al.* 2013b, *MNRAS*, 433, 1991

Steffen, W., Koning, N., Wenger, S., Morisset, C., Magnor, M., *et al.* 2011, *IEEE Transactions on Visualization and Computer Graphics*, Volume 17, Issue 4, p.454–465, 17, 454

https://doi.org/10.1017/S1743921320000216 Published online by Cambridge University Press